

Beyond Contact Tracing: Community-Based Early Detection for Ebola Response

Daniel Cooney, Vincent Wong, and Yaneer Bar-Yam

New England Complex Systems Institute

210 Broadway, Suite 101, Cambridge, MA 02139, USA

(Dated: June 1, 2022)

Abstract

The 2014 Ebola outbreak in west Africa raised many questions about the control of infectious disease in an increasingly connected global society. Limited availability of contact information has made contact tracing difficult or impractical in combating the outbreak. We consider the development of multi-scale public health strategies and simulate policies for community-level response aimed at early screening of communities rather than individuals, as well as travel restrictions to prevent community cross-contamination. Our analysis shows community screening to be effective even at a relatively low level of compliance. In our simulations, 40% of individuals conforming to this policy is enough to stop the outbreak. Simulations with a 50% compliance rate are consistent with the case counts in Liberia during the period of rapid decline after mid September, 2014. We also find the travel restriction policies to be effective at reducing the risks associated with compliance substantially below the 40% level, shortening the outbreak and enabling efforts to be focused on affected areas. Our results suggest that the multi-scale approach could be applied to help end the outbreaks in Guinea and Sierra Leone, and the generality of our model can be used to further evolve public health strategy for defeating emerging epidemics.

I. INTRODUCTION

The initial medical response to Ebola in 2014 focused on caring for individuals in hospital settings and using contact tracing as the primary preventative measure [1]. Contact tracing is the accepted method for public health control of infectious diseases [2]. Under contact tracing, a patient admitted to a hospital is asked about their recent direct contacts, and those contacts are monitored or isolated for the incubation period of the disease [2, 3]. The spread of Ebola to dense urban communities made it difficult or impossible for contact tracing to work. As an alternate approach, we consider community-based monitoring and limiting travel to reduce inter-community contagion [4]. Such approaches were taken in Liberia beginning in mid September 2014 [5, 6] and in Sierra Leone beginning in mid December 2014 [7], and may be responsible for the rapid reduction in cases seen in those two countries. In particular, in early March 2015, it was announced that there were zero remaining active cases of Ebola in Liberia [8]. While the Centers for Disease Control Director Tom Frieden attributed much of the success in the public health effort to the formation of local teams based upon the principle of RITE (Rapid Isolation and Treatment of Ebola) [9], the direct cause of the reduction is not well documented. Here we simulate the progress of an epidemic and found that community monitoring can be highly effective in stopping an outbreak.

In general, early detection of Ebola-like symptoms is necessary for early care of patients with Ebola and limiting new infections. This is due to the extended infectious period and tendency of the disease to become more contagious as it progresses [10, 11]. Contact tracing addresses this, but it is highly dependent on a simple contact structure where the patient knows all the people they interact with, made nearly impossible in urban environments with more than a few cases. Instead of monitoring individuals from a list of contacts, a community-based strategy requires that entire communities be monitored for new cases until infection is ruled out. Symptomatic individuals are isolated and treated to prevent further infections. This community-based early detection is augmented by restricting long-distance travel or subjecting travelers to extended periods of limited contact and observation. Restricting travel inhibits cross-contamination between communities and allows more targeted care to be given to infected communities. The objective is to progressively limit the disease to smaller and smaller areas and to focus resources on the areas in which the disease is present.

If all new infections could be perfectly isolated through the complete monitoring of the population, these policies would evidently drastically limit new Ebola cases and result in an abrupt halt to the epidemic. However, an analysis must account for how effective the implementation of screening will be. It is infeasible and undesirable to constrain the population using high levels of force, so the level of compliance that is achieved is a key variable in efficacy. Here we model compliance as a probability that individuals will adhere to the community-level policies. This captures both the possibility of defiance as well as other sources of performance failure such as accidents or lack of awareness or information. We analyze the level of compliance necessary for the policies to work effectively. As shown in Fig. 1, we find that even with 40% compliance the community level policies curtail the epidemic and a 60% compliance rapidly ends the outbreak.

II. MODEL DETAILS

Our model is a Susceptible, Exposed, Infectious, Removed (SEIR) model on a spatial lattice of individuals (Fig. 2) with periodic boundary conditions. Individuals can be in one of four states: disease-free and never previously infected (susceptible), infected in the latent period without symptoms (exposed), infected with symptoms (infectious), and recovered or dead (removed). Newly infected individuals progress through a latent period for Δ days where they are asymptomatic and not contagious. They then become contagious for a period of Γ days, at the end of which they have either died or have recovered and have acquired immunity from further reinfection. Each individual interacts with all four of its nearest neighbors on the lattice once per day, and an infectious individual infects a susceptible neighbor with probability τ during a given interaction. Each individual also interacts with another randomly chosen individual from the population. If one of them is infectious, they have a probability η of infecting the other by this long-range interaction. A schematic of these interactions is shown in Fig. 2. This mix of local and long-range disease transmission was chosen for our model to reflect the tendency for Ebola to spread both within households and through non-local interactions in shared taxis, hospitals, or through other travel. Additionally, it is known that the presence of even a small probability of long-range disease transmission can allow the rapid spread of an epidemic on a regional or global scale [12].

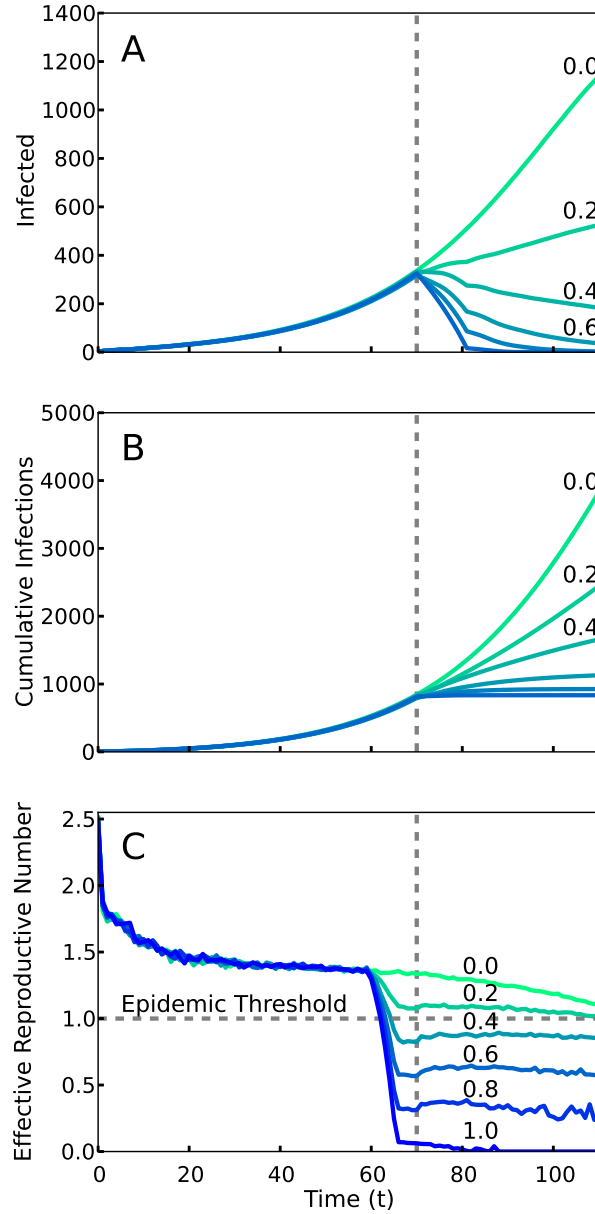


FIG. 1: **Simulations of an outbreak with a community-level screening intervention.** Screening begins at the vertical dotted line, with a level of compliance indicated by label and color (green 0 to blue 1.0). A. Number of cases with or without symptoms. Note that even 40% compliance (0.4) results in decrease in cases. B. Cumulative cases. C. R_t , the effective reproductive number—the average number of individuals infected by an index case at time t . For an epidemic to continue to grow, R_t must exceed 1. For 40% compliance (0.4) and greater, R_t decreases below one, corresponding with a decrease in active cases. R_t drops before $t = 70$ because policies affect the contagion of individuals that are initially infected prior to the intervention.

The community-level public health interventions are modeled based on a proposed policy draft [4] and include daily checks for symptoms and isolation of individuals found to be

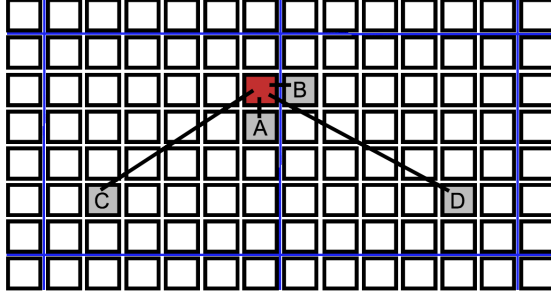


FIG. 2: **Schematic of different types of transmission.** Black squares indicate individuals of a spatially structured population, blue lines denote partitions between communities. A. Neighbor infection within a neighborhood. B. Cross-partition neighbor infection to another community. C. Long-range transmission within a community. D. Long-range transmission across a partition.

in the infectious state. In our simulations, we allowed the disease to spread unabated for the first T_0 days, after which the intervention policies are put into place. The time until the start of the intervention is important in measuring the impact of early response on the control of an emerging outbreak. We assume that, even after the start of the intervention, individuals cannot be isolated and are fully capable of infecting others on the first day of their infectious period. This captures the idea that an individual can become infectious and infect someone else between symptom checks on consecutive days. With probability κ , infectious individuals are chosen to be compliant, which means that, after the first day of their infectious period, they will be perfectly isolated and incapable of interacting with others for the final $\Gamma - 1$ days of their infectious period. The lack of compliance, occurring with probability $1 - \kappa$, is assumed to be complete in the sense that noncompliant individuals continue to infect others for the duration of their infectious period.

The travel restrictions are implemented based on cordons outlined in the policy draft [4]. We subdivide the population into square neighborhoods of equal size classified at each time as one of three types: A , B , or C . The initial type of each neighborhood is determined by monitoring of the population for Γ days upon the onset of the public health intervention. Type A neighborhoods are subpopulations in which at least one resident individual is infectious. Type C neighborhoods are subpopulations for which two criteria have simultaneously been satisfied: there has not been an infectious case in the past Γ days and the neighborhood does not share a border with any neighborhoods of type A . Type B neighborhoods do not have any active infectious cases, but have not yet satisfied the criteria to become a type

C neighborhood. Neighborhoods are updated according to these criteria every timestep, however, we assume that travel restrictions implemented via a dynamic cordon prevent transmission of the disease to type C neighborhoods. This ensures that residents of type C neighborhoods are protected from infection, and renders type C as an absorbing state. The purpose of the classification is to enable a focus of effort on screening neighborhoods of types A and B . Given effective interventions, type A neighborhoods will progressively be reclassified as type B and then as type C , allowing for resources to be devoted to the remaining affected areas and facilitating the goal of reaching zero active cases within the region of intervention.

III. DATA AND PARAMETERS

We used data from the World Health Organization [13] to determine model parameters that match the exponential growth phase of the Ebola outbreak in Liberia. By performing an exponential regression, we determined that the cumulative number of confirmed cases, $y(t)$, in Liberia approximately followed the functional form $y(t) \propto \exp(0.052 t)$, consistent with the analysis done by Chowell and Nishiura [14].

It is useful to consider the value of the basic reproduction number, R_0 , defined as the average number of individuals infected by a single index case in an otherwise susceptible population. R_0 has a clear threshold value for epidemics: outbreaks with $R_0 > 1$ experience exponential growth, whereas outbreaks with $R_0 < 1$ die out exponentially. To deduce R_0 from the exponential growth rate, we used an expression derived from a mean-field version of the SEIR model (see Appendix):

$$R_0 = 1 + (\Delta + \Gamma) r + \Delta \Gamma r^2 \quad (1)$$

where r is the empirically-measured exponential growth rate of the cumulative number of cases [15]. Values for Δ and Γ must be identified in order to obtain a value of R_0 . We consider two different sets of parameter values corresponding to two different estimates of R_0 for the 2014 Ebola outbreak in Liberia.

First, we considered a latency period of $\Delta = 5$ days and an infectious period of $\Gamma = 6$ days to reflect the modeling assumptions of Althaus [16]. Using these time periods and infection

parameters of $\tau = 0.15$ and $\eta = 0.0125$, we conducted 1,000 simulations and obtained an average exponential growth rate of 0.0536, which results in an R_0 estimate of 1.68, comparable to the value 1.59 obtained by Althaus. The values of τ and η were chosen so that long range infections occurred but, as observed in West Africa, local infections dominated. The specific values do not change the conclusions. As Althaus based his parameter values on measurements from a previous outbreak on the same subtype of Ebola [16, 17], the figures presented in the text of the paper are for these parameter values.

Second, we used the parameter values $\Delta = 10$ and $\Gamma = 7$ to compare our model with that of Chowell and Nishiura, who estimated that $R_0 = 1.96$ [14]. Simulating this epidemic with infection parameters of $\tau = 0.18$ and $\eta = 0.015$, we obtained an average exponential growth rate of 0.0505, with a corresponding R_0 value of 2.04, similar to that found by Chowell and Nishiura. These authors based their parameter values on previously hypothesized epidemic properties of Ebola [14, 18]. Results using these parameter values are in the Supplement.

For each set of parameters, we simulated compliances ranging from 0.0 to 1.0 in steps of 0.05, and intervention delay times of 50, 70, 90, and 110. Results are averaged over 1,000 simulations of a population of 10,000 individuals, 100×100 square lattice, with neighborhoods of size 100, 10×10 sublattices, initialized with 0.02% of the population infectious and 0.02% latent.

IV. RESULTS

Fig. 1 shows the number of current and cumulative cases for various levels of compliance with community level interventions implemented at $T_0 = 70$ days and without travel restrictions. We found that a relatively low compliance of 0.4 with the community screening policies was enough to end the outbreak (Fig. 1A). Fig. 1B shows that there is relatively little difference in the cumulative number of infections over the duration of the outbreak for the interventions with 0.6, 0.8, and 1.0 compliance. Thus, and perhaps surprisingly, the greatest gains in reducing the epidemic duration and cumulative number of cases arise from a particularly low level of compliance. Community level responses are highly robust.

The impact of intervention policies can be readily seen by plotting the effective reproduction number R_t , the average number of secondary infections caused by a primary case who is first infected at time t . An R_t greater than 1 at a given time implies that the epi-

demographic will grow exponentially over the short term, while less than one implies it will decline exponentially. Unlike R_0 , R_t is designed to reflect the effect of interventions as well as that of natural epidemic burnout. Plotted in Fig. 1C, we see that compliance levels of 0.6, 0.8, and 1.0 cause the value of R_t to decrease well below the threshold value 1.0 within a span of several days. This represents a quick transition from a regime in which the disease is growing exponentially to a regime in which the epidemic can no longer sustain itself and consequently dies out. Even with a compliance of 0.4, enough infections were halted to reduce the value of R_t below 1 (Fig. 1C).

To observe the effects of the travel restrictions, we show the outbreak length and the cumulative number of infections for interventions implemented at time $T_0 = 70$ with and without the travel restrictions for our simulated compliance values in Figs. 3A and 3B. Without travel restrictions, compliance levels between 20% and 40% actually prolong the outbreak relative to the no intervention case (Fig. 3A). For these levels of compliance community screening slows transmission but insufficiently to halt the outbreak, so transmission continues at a slower rate until the population is exhausted. Travel restrictions greatly reduce this effect. Travel restrictions also noticeably decrease the cumulative number of infections for low levels of compliance (Fig. 3B). This shows that, in the event of low compliance, travel restrictions limit the spread and duration of the outbreak.

Comparing the cumulative cases as a function of compliance for different delay times (Fig. 3C), interventions with an earlier start time T_0 generally result in fewer cumulative infections. However, without travel restrictions, this is much less true for low levels of compliance. Thus, travel restrictions ensure that early policy implementation is effective even at low compliance. Fig. 3C also shows that higher compliances than 0.6 have comparatively little impact on the cumulative number of cases.

We visualized the evolution of neighborhood types over time with the cordon to demonstrate the spatial constriction of the disease with this policy (Fig. 4). The first panel (top left) shows the geographical distribution of neighborhood types shortly after the policies come into effect. The infected area shrinks and the ratio of type A (red) to type B (green) neighborhoods decreases over time.

In Fig. 5 we plot both the reported number of cases in Liberia [19] and our simulation with $T_0 = 50$ days and a 50% compliance (0.5). Our simulations fit the observed case count data in Liberia for the parameters chosen, indicating that the early screening intervention

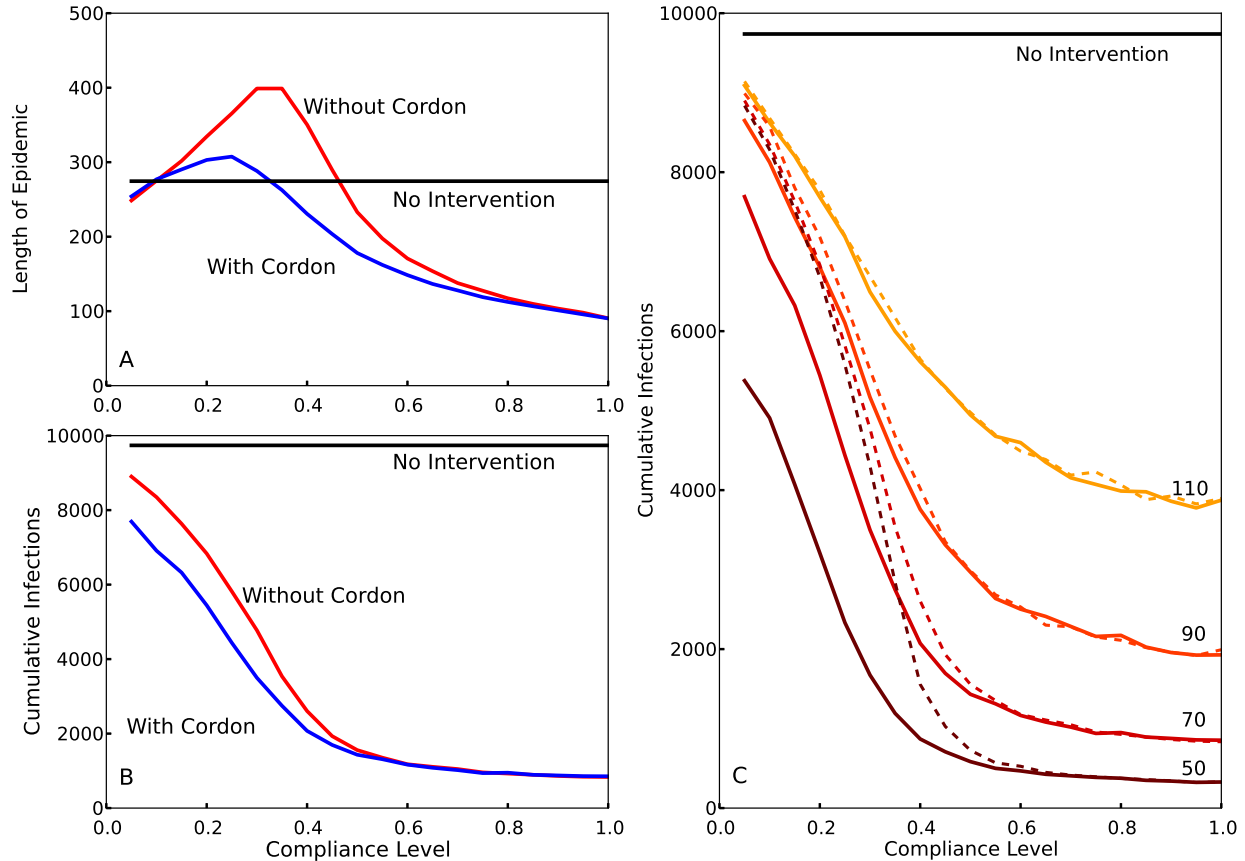


FIG. 3: **Effect of compliance on epidemic length and cumulative infections with and without travel restrictions.** A and B: Blue shows the case with travel restrictions, and red shows the case without such restrictions. Differentiation between the two occurs because the travel restrictions compensate for low levels of compliance. This decreases the length of the epidemic A and reduces the cumulative number of infections B in cases of low compliance. C. The cumulative number of infections over the entire epidemic, as a function of compliance levels and intervention times. Colors from brown to yellow signify intervention times (50, 70, 90, 110). Without enforced travel restrictions (dotted lines), a low compliance results in little differentiation between early and late policy implementation. The travel restrictions (solid lines) dramatically reduce infection number for earlier interventions at low compliance.

was far from complete, but was sufficiently effective. Since the results of the simulation are robust to variation in parameters, the correspondence of the real world data in with the simulation reflects the reduction of R_t below the epidemic threshold Liberia.

We note that recent research on contagious processes on networks that are not geographically local have considered heterogeneous connectivities across nodes, and specifically power law node connectivity. Under these conditions highly connected nodes enable the disease to spread across the entire network at arbitrarily low contagion rates [20]. Cordons that

restrict the contagion by limiting geographical spread would also impose a cutoff on power law connectivities leading to a non-zero threshold contagion rate for such networks.

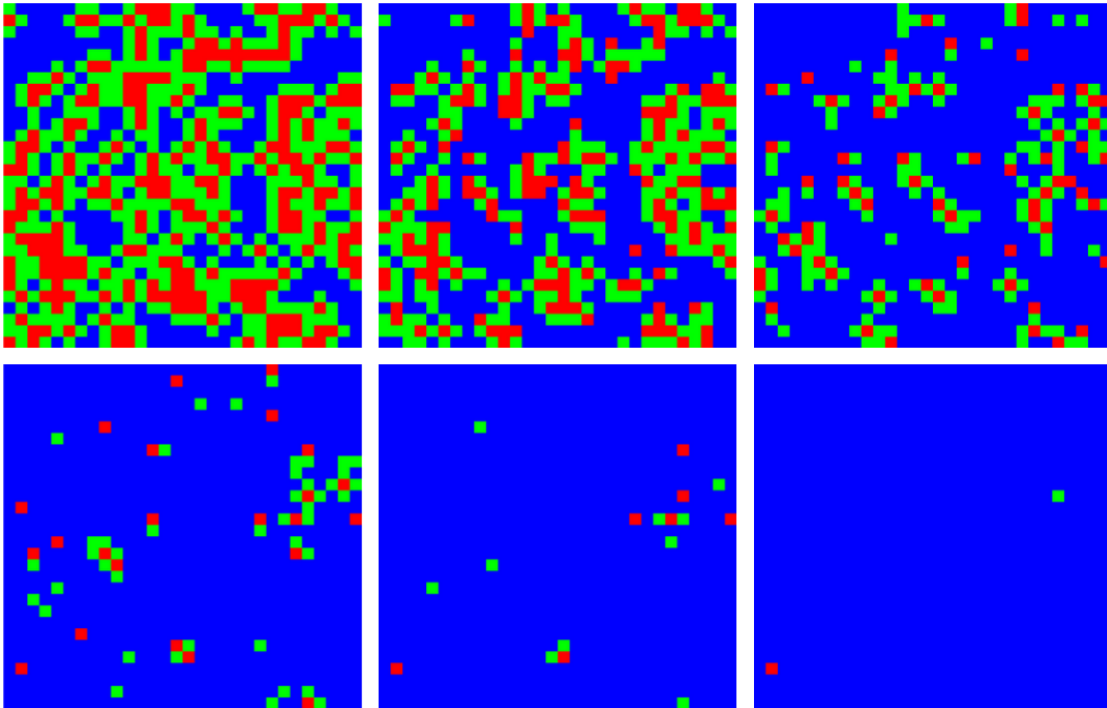


FIG. 4: **Contraction of the epidemic areas using cordons and labeled neighborhoods.** A simulated epidemic run on a 300×300 lattice with neighborhoods of size 10×10 , with 70% compliance (0.7) and a delay of $T_0 = 50$ days. Colored squares represent neighborhoods of types A (red, known infection), B (green, neighboring known infection), and C (blue, neither A nor B). Top (left to right) 60, 70, and 80 days, bottom 90, 100, and 110 days. Type C neighborhoods remain free from infection due to the protection provided by travel restrictions.

V. CONCLUSIONS

We found that a policy of community response can be effective at combating disease outbreaks without relying on information about infected individual's contact networks. This highlights the possibility of alternate methods of combating outbreaks without contact tracing. We have shown the policies require a surprisingly low compliance to end the outbreak. Notably, we see that for estimated Ebola parameters, 40% compliance is sufficient, and the cumulative number of infections in an outbreak is not substantially decreased by compliance higher than 60%. We also found that travel restrictions can be used to reduce the risks associated with compliance below 40%, and that the pairing of community-level interventions

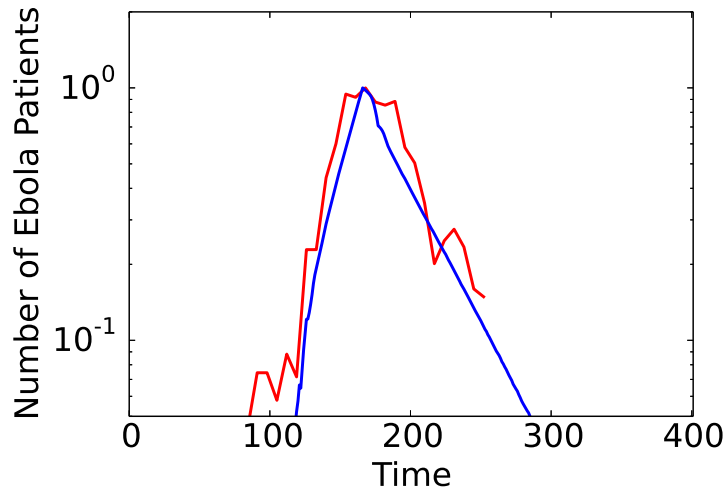


FIG. 5: **Comparison of empirical data with simulations** Normalized, linear-log plot of Liberia empirical values (red) compared with simulation data (blue) with $T_0 = 50$ and 50% compliance (0.5).

and travel restrictions can result in saving a substantial fraction of individuals from infection at any level of compliance. Public health interventions implementing variants of these policies have helped the number of active Ebola cases to reach zero in Liberia in March 2015 [8, 9]. Our results provide further evidence that community-level interventions and travel restrictions may be useful in ending the still active outbreaks in Guinea and Sierra Leone.

Acknowledgments

We thank Irving Epstein, Joseph Norman, Francisco Castrillo, Alfredo Morales, and Matthew Hardcastle for comments on the manuscript and Joa Ja'keno Okech-Ojony for description of community interventions in Liberia.

-
- [1] World Health Organization (2014). Contact tracing during an outbreak of Ebola virus disease. Available at <http://www.who.int/csr/resources/publications/ebola/contact-tracing/en>. Accessed March 31, 2015.
- [2] World Health Organization (2014). Frequently asked questions on Ebola virus disease. Available at <http://www.who.int/csr/disease/ebola/faq-ebola/en>. Accessed March 31, 2015.
- [3] Centers for Disease Control and Prevention (2014). Ebola factsheet. Available at <http://www.cdc.gov/vhf/ebola/pdf/ebola-factsheet.pdf>. Accessed March 31, 2015.
- [4] Bar-Yam Y (2014) DRAFT New Ebola response strategy: Local care team early detection response, *New Engl Complex Syst Inst* (Oct. 12). Available at <http://necsi.edu/research/management/health/ebolaresponse.html>. Accessed March 31, 2015.
- [5] Bar-Yam Y (2014) Is The Response in Liberia Succeeding? Positive indications. *New Engl Complex Syst Inst* (Oct. 17). Available at <http://necsi.edu/research/social/pandemics/liberiadecrease.html>. Accessed April 2, 2015.
- [6] World Health Organization (2014). Liberia succeeds in fighting Ebola with local, sector response. Available at <http://who.int/features/2015/ebola-sector-approach/en/>. Accessed April 27, 2015.
- [7] Associated Press (2014) Ebola outbreak: Sierra Leone officials going door to door. *CBS News* (Dec. 17). Available at <http://www.cbsnews.com/news/ebola-outbreak-sierra-leone-officials-going-door-to-door>. Accessed March 31, 2015.
- [8] Onishi H (2015). Last known Ebola patient in Liberia is discharged. *The New York Times* (March 5). Available at <http://www.nytimes.com/2015/03/06/world/africa/last-ebola-patient-in-liberia-beatrice-yardolo-discharged-from-treatment.html>. Accessed March 31, 2015.
- [9] Frieden T (2015) Rapid Detection and Response Are Essential to Stopping Ebola. *The Huffington Post* (Feb. 18). Available at http://www.huffingtonpost.com/tom-frieden-md-mp/rapid-detection-and-respo_b_6705258.html. Accessed March 31, 2015.
- [10] Yamin D, Gertler S, Ndeffo-Mbah ML, Skrip LA, Fallah M, Nyenswah TG, Altice FL, Galvani AP (2015) Effect of ebola progression on transmission and control in liberia. *Ann Intern Med* 162(1): 11-17.
- [11] Brauer F (2005) Age of infection in epidemiology models. *Electronic Journal of Differential*

- Equations*. Volume 12. Available at <http://147.91.102.6/EMIS/journals/EJDE/Volumes/conf-proc/12/b2/brauer.pdf>. Accessed March 3, 2015.
- [12] Rauch EM, Bar-Yam Y (2006) Long-range interactions and evolutionary stability in a predator-prey system. *Phys Rev E* 72(2): 020903.
- [13] World Health Organization (2014). Ebola response roadmap. Available at <http://www.who.int/csr/resources/publications/ebola/response-roadmap/en>. Accessed March 31, 2015.
- [14] Chowell G, Nishiura H, Bettencourt LM (2007) Comparative estimation of the reproduction number for pandemic influenza from daily case notification data. *J R Soc Interface* 4(12): 155-166.
- [15] Lipsitch M, et al. (2003) Transmission dynamics and control of severe acute respiratory syndrome. *Science* 300(5627): 1966-1970.
- [16] Althaus CL (2014) Estimating the reproduction number of ebola virus (EBOV) during the 2014 outbreak in west africa. *PLoS Curr* 1. doi: 10.1371/currents.outbreaks.91afb5e0f279e7f29e7056095255b288.
- [17] WHO Ebola Response Team (2014) Ebola virus disease in west africa the first 9 months of the epidemic and forward projections. *N Engl J Med* 371(16): 1481-95.
- [18] Lekone PE, Bärbel FF (2006) Statistical inference in a stochastic epidemic SEIR model with control intervention: ebola as a case study. *Biometrics* 62(4): 1170-1177. DOI: 10.1111/j.1541-0420.2006.00609.x
- [19] World Health Organization (2015) Ebola data and statistics. Available at <http://apps.who.int/gho/data/node. ebola-sitrep>. Accessed March 31, 2015.
- [20] Pastor-Satorras R, Vespignani A (2001) Epidemic spreading in scale-free networks. *Phys Rev Lett* 86(14): 3200.
- [21] Keeling MJ, Rohani P (2008) Modeling infectious diseases in humans and animals. *Princeton University Press*.
- [22] Barbara J, et al. (2001) Large-scale quarantine following biological terrorism in the united states: Scientific examination, logistic and legal limits, and possible consequences. *JAMA* 286(21): 2711-2717.
- [23] Burke DS, et al. (2006) Individual-based computational modeling of smallpox epidemic control strategies. *Acad Emerg Med* 13(11): 1142-1149.

- [24] Colizza V, Vespignani A (2008) Epidemic modeling in metapopulation systems with heterogeneous coupling pattern: Theory and simulations. *J Theor Biol* 251(3): 450 - 467.
- [25] Wallinga J, Lipsitch M (2007) How generation intervals shape the relationship between growth rates and reproductive numbers. *Proc Biol Sci* 274(1609): 599 - 604.
- [26] Ball F, Mollison D, Scalia-Tomba G (1997) Epidemics with two levels of mixing. *Ann Appl Probab* 7(1): 46-89.
- [27] Keeling MJ, Eames KT (2005) Networks and epidemic models. *J R Soc Interface* 2(4): 295-307.
- [28] Eames KT, Keeling MJ (2002) Modeling dynamic and network heterogeneities in the spread of sexually transmitted diseases. *Proc Natl Acad Sci U S A* 99(20): 13330-13335.
- [29] Keeling MJ (1999) The effects of local spatial structure on epidemiological invasions. *Proc R Soc Lond B Biol Sci* 266(1421): 859-867.
- [30] Frank B, David S, Pieter T (2009) Threshold behaviour and final outcome of an epidemic on a random network with household structure. *Adv Appl Probab* 41(3): 765-796.
- [31] Bonaccorsi S, Ottaviano S, De Pellegrini F, Socievole A, Van Mieghem P (2014) Epidemic outbreaks in two-scale community networks. *Phys Rev E* 90(1): 012810.
- [32] Kiss IZ, Green DM, Kao RR (2006) Infectious disease control using contact tracing in random and scale-free networks. *J R Soc Interface* 3(6): 55-62.
- [33] Klinkenberg D, Fraser C, Heesterbeek H (2006) The effectiveness of contact tracing in emerging epidemics. *PloS One* 1(1): e12.
- [34] Longini IM, et. al. (2005) Containing pandemic influenza at the source. *Science* 309(5737): 1083-1087.
- [35] Rothstein MA, et al. (2003) Quarantine and Isolation: Lessons learned from SARS. *University of Louisville School of Medicine, Institute for Bioethics, Health Policy and Law*. doi: 10.3201/eid1902.120312.
- [36] Schabas R (2004) Severe acute respiratory syndrome: Did quarantine help? *Can J Infect Dis Med Microbiol* 15(4): 204.
- [37] Tognotti E (2013) Lessons from the history of quarantine, from plague to influenza A. *Emerg Infect Dis* 19(2): 254.
- [38] Sun C, Hsieh YH (2010) Global analysis of an seir model with varying population size and vaccination. *Appl Math Model* 34(10): 2685-2697.

- [39] Colizza V, Barrat A, Barthelemy M, Valleron AJ, Vespignani A (2007) Modeling the worldwide spread of pandemic influenza: baseline case and containment interventions. *PLoS Med* 4(1): e13.
- [40] López L, Giovanini L, Burguener G (2014) Addressing population heterogeneity and distribution in epidemics models using a cellular automata approach. *BMC Res Notes* 7(1):234.
- [41] Fuentes MA, Kuperman MN (1999) Cellular automata and epidemiological models with spatial dependence. *Physica A* 267(3): 471-486.
- [42] Eubank S, et. al. (2004) Modelling disease outbreaks in realistic urban social networks. *Nature* 429(6988): 180-184.
- [43] Fraser C, Riley S, Anderson RM, Ferguson NM (2004) Factors that make an infectious disease outbreak controllable. *Proc Natl Acad Sci U S A* 101(16): 6146-6151.
- [44] Read JM, Eames KT, Edmunds WJ (2008) Dynamic social networks and the implications for the spread of infectious disease. *J R Soc Interface* 5(26): 1001-1007.
- [45] Eames KT, Keeling MJ (2003) Contact tracing and disease control. *Proc R Soc Lond B Biol Sci* 270(1533): 2565-2571.
- [46] Riley S, Ferguson NM (2006) Smallpox transmission and control: spatial dynamics in great britain. *Proc Natl Acad Sci U S A* 103(33): 12637-12642.
- [47] Huerta R, Tsimring LS (2002) Contact tracing and epidemics control in social networks. *Phys Rev E* 66(5): 056115.
- [48] Kiss IZ, Green DM, Kao RR (2005) Disease contact tracing in random and clustered networks. *Proc R Soc Lond B Biol Sci* 272(1570): 1407-1414.
- [49] Stadler T, Kühnert D, Rasmussen DA, du Plessis L (2014) Insights into the early epidemic spread of ebola in sierra leone provided by viral sequence data. *PLoS Curr* 6. doi: 10.1371/currents.outbreaks.02bc6d927ecee7bbd33532ec8ba6a25f.
- [50] Chowell G, Hengartner NW, Castillo-Chavez C, Fenimore PW, Hyman JM (2004) The basic reproductive number of ebola and the effects of public health measures: the cases of congo and uganda. *J Theor Biol* 229(1): 119-126.
- [51] Heffernan JM, Smith RJ, Wahl LM (2005) Perspectives on the basic reproductive ratio. *J R Soc Interface* 2(4): 281-293.
- [52] Nishiura H, Chowell G (2014) Early transmission dynamics of ebola virus disease (EVD), West Africa, March to August 2014. *Euro Surveill* 19(36): 20894.

- [53] Chowell G, Nishiura H (2014) Transmission dynamics and control of ebola virus disease (EVD): a review. *BMC Med* 12(1):196.
- [54] Nishiura H, Chowell G (2015) Theoretical perspectives on the infectiousness of ebola virus disease. *Theor Biol Med Model* 12(1). doi:10.1186/1742-4682-12-1
- [55] Gomes MF, y Piontti AP, Rossi L, Chao D, Longini I, Halloran ME, Vespignani A (2014) Assessing the international spreading risk associated with the 2014 west african ebola outbreak. *PLOS Curr* 1. doi: 10.1371/currents.outbreaks.cd818f63d40e24aef769dda7df9e0da5.
- [56] Tsimring LS, Huerta R (2003) Modeling of contact tracing in social networks. *Physica A* 325(1): 33-39.
- [57] Stadler T, Kühnert D, Rasmussen DA, du Plessis L (2014) Insights into the early epidemic spread of ebola in sierra leone provided by viral sequence data. *PLoS Curr* 6:currents.outbreaks.02bc6d927ecee7bbd33532ec8ba6a25f.
- [58] Towner JS, et. al. (2004) Rapid diagnosis of ebola hemorrhagic fever by reverse transcription-pcr in an outbreak setting and assessment of patient viral load as a predictor of outcome. *J Virol* 78(8): 4330-4341.
- [59] World Health Organization (2014). Ebola virus disease. Available at <http://www.who.int/mediacentre/factsheets/fs103/en/> Accessed April 15, 2015.
- [60] Hunter JD (2007) Matplotlib: A 2d graphics environment. *Comput Sci Eng* 9(3): 90-95.

APPENDIX

A. SEIR Model

We model Ebola using a Susceptible, Exposed, Infectious, Removed (SEIR) model with a finite, spatially structured population with periodic boundary conditions. In an SEIR model, each individual can be in one of four states of health:

S (susceptible): Healthy and capable of being infected.

E (exposed): Infected but asymptomatic and incapable of transmitting the illness, otherwise referred to as latently infected.

I (infectious): Infected and symptomatic. Capable of infecting susceptible individuals.

R (removed): No longer symptomatic, infectious, or infectable. This state includes both individuals that have survived and gained immunity, and those who have died.

Individuals transition from state to state in the order $S \rightarrow E \rightarrow I \rightarrow R$. Historically, the case-fatality rate for Ebola outbreaks has been around 50% [59], so the number of removed individuals can be divided by two to obtain an estimate of the number of deaths.

The standard non-spatial SEIR model is governed by a nonlinear system of differential equations. Let S , E , I , and R represent the number of individuals in the corresponding states, then

$$\begin{aligned}\frac{dS}{dt} &= -\alpha SI \\ \frac{dE}{dt} &= \alpha SI - \delta E \\ \frac{dI}{dt} &= \delta E - \gamma I \\ \frac{dR}{dt} &= \gamma I\end{aligned}\tag{2}$$

where δ represents the rate at which exposed individuals become infectious and γ represents the rate at which the disease removes infectious individuals (either via death or survival with acquired immunity) [21]. Transmission of the disease requires contact between individuals in state I and state S . The infection rate parameter α is usually rewritten as $\frac{\kappa\tau}{N}$, where each susceptible individual has τ interactions with any of the N other members of population with probability κ of being infected by an infectious one [21].

This system of differential equations provides a mean-field representation of the dynamics of an epidemic with an SEIR structure. We consider potential policy recommendations that involve explicit change of the contact network structure of the population. For our purpose, a model based upon this mass-action system of differential equations is insufficient.

B. Spatial Model

We model a population on a square lattice where each individual has three properties: their current state of health (S , E , I , or R), the amount of time for which they have been in that state, and whether or not they are compliant with community-level policies. If an individual is characterized as compliant, then they can be successfully isolated after entering the infectious state.

Using the definitions from the SEIR model, we consider the rate of transition from state E to state I to be δ and the rate of transition from state I to state R as γ . For simplicity, individuals transition deterministically from state E to state I (from state I to state R) after $\Delta = \frac{1}{\delta}$ ($\Gamma = \frac{1}{\gamma}$) time steps. We take Δ and Γ to be integer numbers of days so that we can choose each time step of the simulation to represent a single day.

We initialized the population by randomly setting 0.02% of the individuals to be in each of states E and I , with the remaining individuals starting out in state S . Each individual was designated as compliant with probability κ . All individuals seeded in state I were initialized at the beginning of the infectious period, and individuals seeded in state E were given a random number between Δ and $\frac{3}{5}\Delta$ days remaining in the latent period. We chose 0.02% and the initial compartment times in order to smoothly simulate the epidemic growth. Simulations with different small initial numbers of seed cases and seeded state times yielded essentially the same behavior.

The transmission of the disease involves both local and long-range spreading mechanisms. Each infectious individual has probability τ of infecting each of its susceptible neighbors during a given day. Additionally, each susceptible individual chooses at random an individual on the grid with whom they will interact on a given day and, if infectious, the susceptible will become infected with probability η .

C. Spatial model R_0

The basic reproduction number, R_0 , is generally defined as the expected number of individuals that a single seeded individual in state I will infect if the rest of the population is susceptible. For large population size G , the R_0 value of this process, with infectious period Γ and number of neighbors ($z = 4$), is approximately given by

$$R_0 \approx \Gamma\eta + z \left(1 - (1 - \tau)^\Gamma\right) \quad (3)$$

The number of neighbors that are infected is given by the second term, and the number of non-neighbors that are infected is given by the first term. The number of neighbors that become infected is complicated by the reduction in number of susceptible neighbors as they become infected from day to day during the infectious period. For the long range interactions, the effect is small due to the large number of possible sites so that a few new infections do not affect the number of susceptible individuals the long range interactions can affect.

To obtain equation 3, consider a neighbor that can be infected by the local infection process with probability τ and independently, by the long-range infection mechanism with probability $\frac{\eta}{G^2}$. The probability that the neighbor is not infected on a given day is $(1 - \tau) \left(1 - \frac{\eta}{G^2}\right)$. An individual is infectious for Γ days after becoming infected. This means that the probability of a particular neighbor being infected is

$$1 - \left((1 - \tau) \left(1 - \frac{\eta}{G^2}\right)\right)^\Gamma = 1 - (1 - \tau)^\Gamma \left(1 - \frac{\eta}{G^2}\right)^\Gamma \quad (4)$$

For z neighbors that can be independently infected (periodic boundary conditions ensure any such individual has the same number of neighbors), the number of infected neighbors is (neglecting corrections of $O(1/G^2)$)

$$z \left(1 - (1 - \tau)^\Gamma \left(1 - \frac{\eta}{G^2}\right)^\Gamma\right) = z \left(1 - (1 - \tau)^\Gamma + O\left(\frac{1}{G^2}\right)\right) \quad (5)$$

For large G the number of infected individuals in the neighborhood is thus $z \left(1 - (1 - \tau)^\Gamma\right)$.

Individuals outside of the infected individual's neighborhood can only be infected by long-range interaction. Neglecting corrections of $O(1/G^2)$, the infected individual chooses

one such individual to visit and infects that individual according to the probability η . Since it is assumed that the concentration of infected individuals is small, the average number of individuals infected is η . The additional infection is only 1 in G^2 , which doesn't affect the calculation in the next period, so the total number over the infectious period is $\Gamma\eta$.

We note that the characterization of R_0 differs from the differential equation SEIR (mean field) model. Since an individual locally infected by the first seeded case has that seeded case as a neighbor, the expected number of susceptible neighbors is less than the seeded case. Therefore, it is unjustified to assume the calculation of R_0 for the first individual holds for the rest of the contagion.

The dynamics of the epidemic can be more completely described by the effective reproduction number, R_t , defined as the average number of secondary infections caused by an index case that is infected at time t . This includes the effect of the reduction of the number of susceptible individuals (epidemic burnout) and susceptible neighbors [12] as well as the impact of the community-level intervention at varying levels of compliance. R_t can be approximated by

$$R_t \approx \Gamma\eta s_t + z_t (1 - (1 - \tau)^\Gamma) \quad (6)$$

where z_t is the average number of susceptible neighbors for an individual infected at time t and s_t is the proportion of susceptible individuals in the whole population. Eq. 6 reduces to Eq. 3 if a susceptible population is seeded with a single infectious individual, as $s_t \approx 1$ and $z_t = z$, which is an individual's neighborhood size in the given population structure.

In Fig. 6, we compare the empirically measured time-series of values for R_t with the time-series of R_t generated by Eq. 6 using empirical values of z_t and s_t averaged over 1,000 simulations with $\Delta = 5$, $\Gamma = 6$, $\tau = 0.15$, and $\eta = 0.0125$ and no public health intervention. Eq. 6 agrees well with the empirically measured values of R_t . The empirically measured value of R_t for $t = 0$ (2.52) is consistent with Eq. 3 (2.57).

D. Model Parameters and Epidemiological Analysis

In order to make relevant comparisons between the results of our simulations and the actual 2014 Ebola outbreak, it is useful to choose model parameters so that the spread of our simulated epidemic matches the real-world spread of Ebola. We chose parameters so

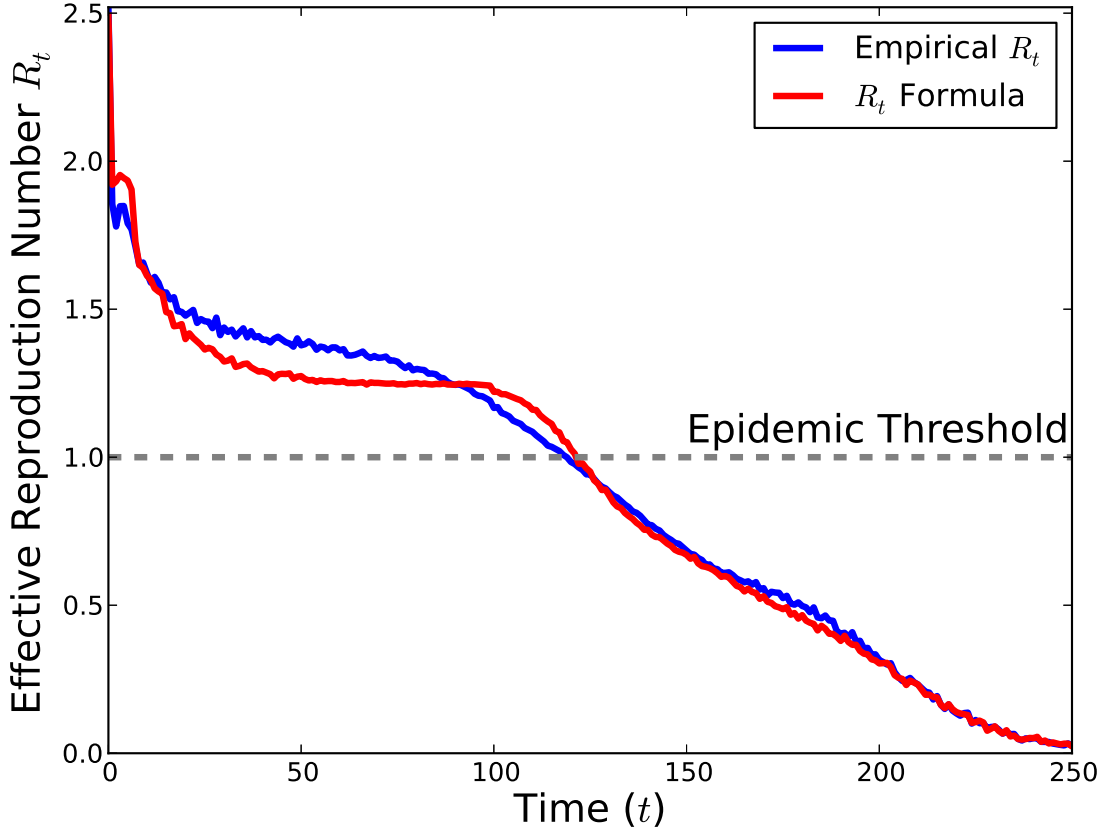


FIG. 6: **Comparison of R_t .** The value of R_t measured from the average number of secondary infections caused by an individual infected at time t , averaged over 1,000 simulations, is shown in blue. R_t calculated by Eq. 6 is shown in red. The values of z_t and S_t , the average number of susceptible neighbors for an individual infected at time t and the average number of susceptibles in the population at time t , are also obtained from an average over 1,000 simulations.

that the simulated epidemic matches the growth of cumulative case numbers observed in the Liberia outbreak. In addition, we consider values of Δ and Γ consistent with the actual mean latent and infectious periods for Ebola. Given these values of Δ and Γ , we find values of the infection parameters τ and η so that the growth rate of cumulative cases in the simulated epidemic is consistent with the actual outbreak.

Given a time series of cumulative cases, $x(t)$, one can estimate the rate of initial exponential growth from a fit to the expression $\ln(x(t)) = b + \lambda t$ [14]. Using data from the World Health Organization, we find $\lambda = 0.052$ for the 2014 outbreak in Liberia, consistent with the value computed by Chowell and Nishiura [53].

We consider two sets of Δ and Γ that have been used to describe the Ebola outbreak. First, we use $\Delta = 5$, $\Gamma = 6$, approximating values of Althaus [16] ($\Delta = 5.3$, $\Gamma = 5.61$) taken from a previous Ebola outbreak with similar immunological properties. We found that this Γ and Δ , when paired with infection parameters $\tau = 0.15$ and $\eta = 0.0125$, produced a Liberia-like exponential growth rate of 0.0536. The results from simulations with these parameter values can be found in the main paper.

We also considered the values $\Delta = 10$, $\Gamma = 7$, which are consistent with the values used by Chowell and Nishiura [53] ($\Delta = 10.1$, $\Gamma = 6.5$), who used hypothesized parameter values proposed by Lekone and Finkenstadt [18, 53]. Using infection parameters of $\tau = 0.18$ and $\eta = 0.015$, our simulated epidemic with this Δ and Γ produced an exponential growth rate of 0.0505, which also roughly matches the exponential growth rate in Liberia. Results from these simulations can be found later in the appendix.

It is common to characterize simulated and real-world outbreaks using R_0 , the average number of secondary infectious caused by a single infectious individual in an otherwise susceptible population. One can obtain an expression for R_0 in terms of Δ , Γ , and λ , the empirically observable exponential growth rate of cumulative cases, through a linear stability analysis of the mean field SEIR model.

The cumulative number of cases $x(t)$ satisfies $x(t) \propto e^{\lambda t}$ near the disease-free equilibrium, where λ is the dominant eigenvalue of the Jacobian matrix obtained from linearizing Eq. 2 around the disease free equilibrium (i.e. where $E = I = R = 0$ and $S = N$) [14, 15, 50, 51]. It can be shown that R_0 is equal to

$$R_0 = 1 + (\Delta + \Gamma) \lambda + (\Delta\Gamma) \lambda^2 \tag{7}$$

Using Eq. 7 and the exponential growth rates generated from our simulations, we see that R_0 is approximately equal to 1.68 for the $\Delta = 5$, $\Gamma = 6$ simulations, and is equal to 2.04 for the $\Delta = 10$, $\Gamma = 7$ case. These values of R_0 agree well with the values of 1.59 and 1.96 estimated by Althaus [16] and by Chowell and Nishiura [53], respectively. This provides further confirmation that our simulated epidemics display similar exponential growth behavior to the 2014 outbreak in Liberia.

E. Results for $\Delta = 10, \Gamma = 7$

We simulated our epidemic with the parameters values $\Delta = 10, \Gamma = 7, \tau = 0.18,$ and $\eta = 0.015$. As shown in Figs. 7 and 8, the qualitative behavior of the epidemic and the impact of intervention policies were similar to the $\Delta = 5, \Gamma = 6$ case. For compliances of 0.6, 0.8, and 1.0, the outbreak ended quickly after the implementation of community-level isolation policies (Fig. 1A), and the value of R_t dropped well below 1 after a few days. The primary difference between this case and the one reported in the main paper can be seen in Fig. 7C where R_t remains near 1 for a long period of time for 0.4 compliance (compare Fig. 7A).

From Fig. 8C, we see that a compliance of 0.6 or higher limits the number of cumulative infections, and that travel restrictions still substantially help to limit the loss of life in the case of low compliance. Early implementation of the intervention (lower values of T_0) results in lower infection totals. However, we also see that cumulative case counts without travel restrictions (dotted lines) only begin to coincide with those with travel restrictions (solid lines) at higher levels of compliance than in the $\Delta = 5, \Gamma = 6$ case. This implies that the travel restrictions provide benefit at higher levels of compliance for these parameter values. Since these parameter values reflect a higher R_0 value (2.04) than the $\Delta = 5, \Gamma = 6$ case, this suggests that travel restrictions are more critical to halting outbreaks of more virulent diseases, as is to be expected.

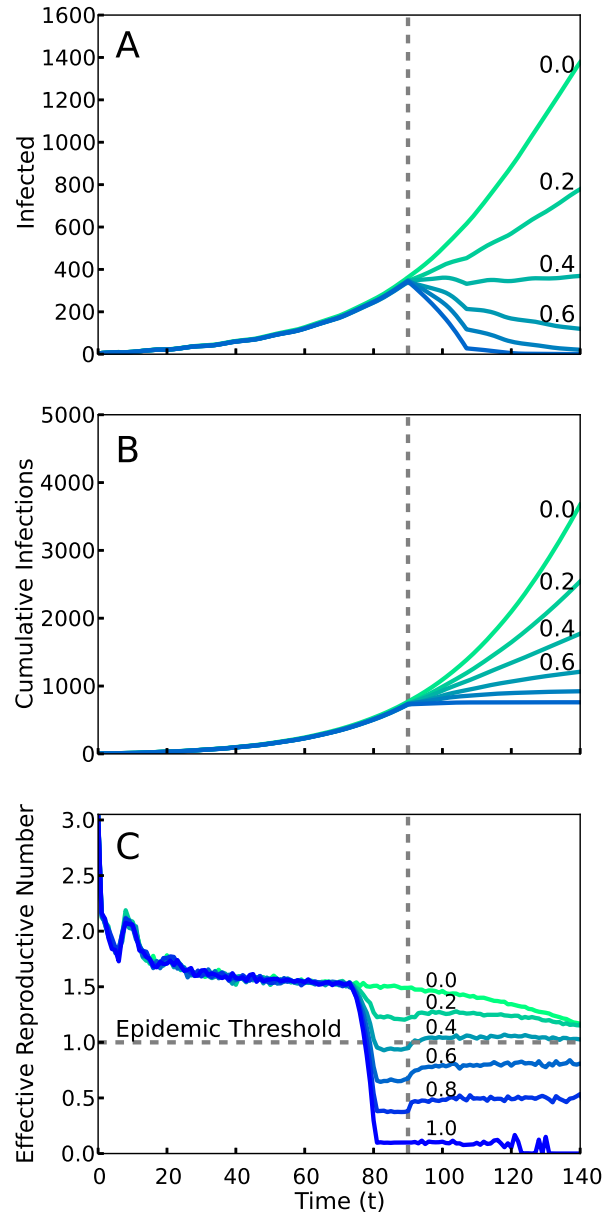


FIG. 7: **Simulations of an outbreak with a community-level screening intervention.** Screening begins at the vertical dotted line, with a level of compliance indicated by label and color (green 0 to blue 1.0). A. Number of cases with or without symptoms. Note that, compared to the simulations in the main paper, 40% compliance (0.4) is no longer sufficient to end this more virulent outbreak. B. Cumulative cases. C. For greater than 40% compliance (0.4), R_t decreases below one, corresponding to a rapid decrease in active cases. Despite this change, the overall results are robust as a compliance value of 0.6 is sufficient to end the outbreak.

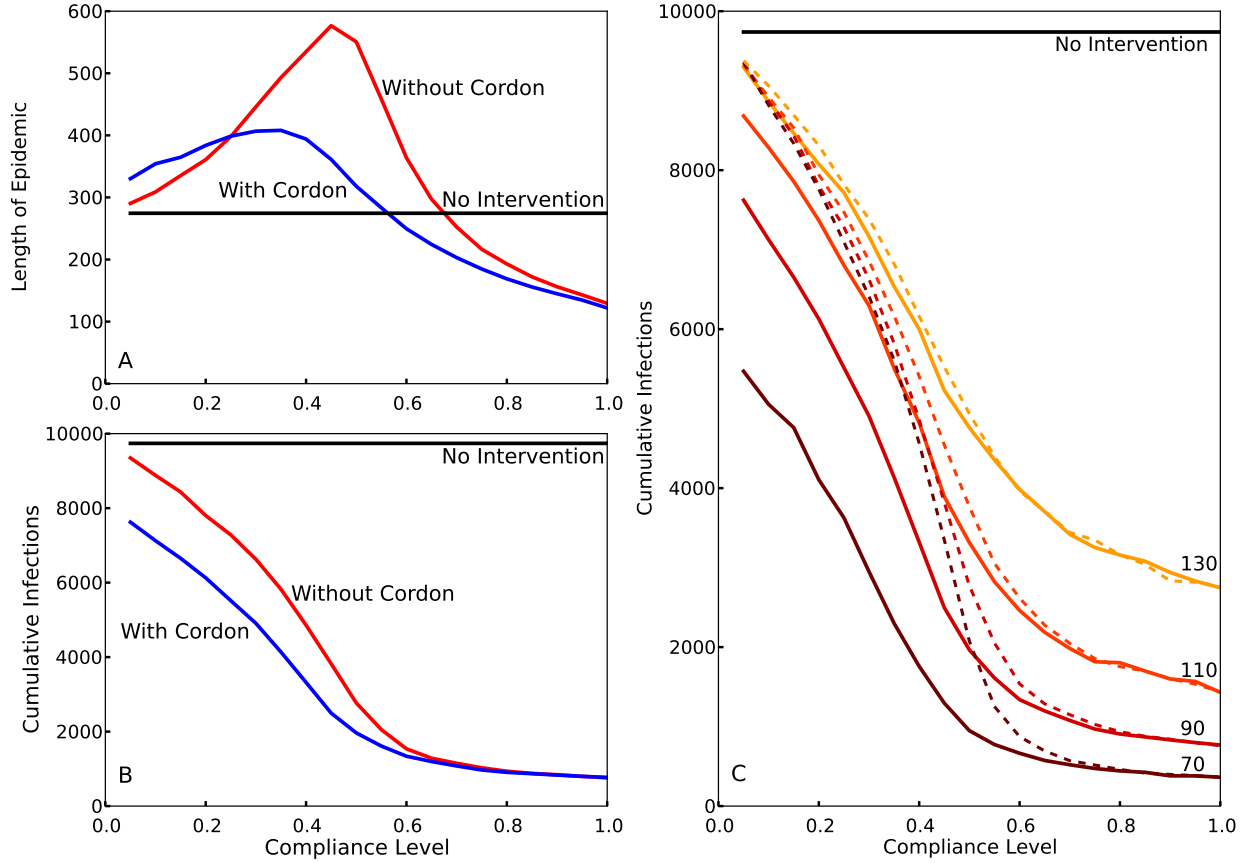


FIG. 8: **Effect of compliance on epidemic length and cumulative infections with and without travel restrictions for the second set of parameter values ($\Delta = 10$, $\Gamma = 7$).** A,B. Simulations with (blue) and without (red) travel restrictions. The travel restrictions compensate for low levels of compliance, and their differences are comparable to Fig. 3 in the main paper. C. The cumulative number of infections over the entire epidemic, as a function of compliance levels and intervention times. Colors from brown to yellow signify intervention times (70, 90, 110, 130). Without enforced travel restrictions (dotted lines), a low compliance results in minimal differences between early and late policy implementation. Travel restrictions (solid lines) dramatically reduce infection numbers for earlier interventions at low compliance. We chose a slightly later set of intervention times T_0 for this set of parameters because the mean generation length ($\Delta + \Gamma$) is about 50% longer, 17 days, compared to the 11 days for the $\Delta = 5$, $\Gamma = 6$ case, so the exponential growth phase begins at a later time.